CHAPTER IV
RESULTS AND DISCUSSION

4.1 Catalyst Characterization

4.1.1 BET Surface Areas and Degrees of Metal Dispersion

BET surface areas and degrees of metal dispersion of the catalysts investigated are shown in Table 4.1. The surface area of $Ce_{0.75}Zr_{0.25}O_2$ (CZO) support is ca. 92 m^2/g whereas those of the others are in the range of 38–71 m^2/g. By loading Ni metal onto CZO support, the CZO surface area was found to decrease by about 23%. This might be because nickel could perform as a nucleating agent to promote the sintering over CZO supported catalysts (Montoya *et al.*, 2000). Moreover, the surface areas were found to decrease with increasing MgO loading. When MgO loading was increased from 5 to 15 wt%, 15Ni/CZO surface areas were decreased to about 46%, probably due to the pore blockage of MgO (Yejun *et al.*, 2007). At a given loading of MgO, the sequential incipient wetness impregnation catalysts showed slightly higher surface area than the co-impregnation catalysts. This suggests that the metal loaded for the sequential incipient wetness impregnation catalysts is uniformly dispersed better than that of the co-impregnation catalysts. At reducing temperature of 500 °C, the metal dispersions were found to decrease with increasing MgO loading. Since no hydrogen chemisorption is observed over the CZO and MgO/CZO, this indicates that Ni atoms being exposed to H_2 were partially covered by MgO. Moreover, the metal dispersion degree for 15Ni/CZO was drastically decreased with increasing the reducing temperature (up to 750 °C). This is probably due to the sintering of Ni particles at high temperatures. However, the metal dispersion degree for 15Ni5Mg/CZO (S) was slightly increased but that for 15Ni5Mg/CZO (C) was slightly decreased with increasing the reducing temperature (up to 750 °C). This suggests that the addition of Mg can stabilize the dispersion degree of Ni particles and retard the sintering of active Ni particles at high temperatures.

Table 4.1 BET surface areas and degrees of metal dispersion of the catalysts

Catalyst	BET surface area (m^2/g)	Metal dispersion[a] (%)	Metal dispersion[b] (%)
CZO	91.60	n/a	n/a
15Ni/CZO	70.69	6.15	0.47
15Ni5Mg/CZO (S)	53.49	3.48	4.01
15Ni5Mg/CZO (C)	46.10	3.31	2.55
15Ni10Mg/CZO (S)	44.24	1.84	n/a
15Ni10Mg/CZO (C)	42.46	1.31	n/a
15Ni15Mg/CZO (S)	38.61	0.89	n/a
15Ni15Mg/CZO (C)	38.19	0.84	n/a

a = Calcined at 500 °C and reduced at 500 °C, b = Calcined at 500 °C and reduced at 750 °C

(S) = Sequential incipient wetness impregnation catalysts

(C) = Co-impregnation catalysts

4.1.2 Temperature-programmed Reduction by Hydrogen (H_2-TPR)

H_2-TPR profiles for the catalysts are presented in Figure 4.1. The TPR profile for CZO indicates a typical reduction peak of CeO_2 at ca. 550 °C. The 15Ni/CZO catalyst possesses two reduction peaks at ca. 320 and 420 °C, and one shoulder peak at about 550 °C. The first peak was attributed to the reduction of free NiO particles interacting weakly with support, and the second peak was attributed to the reduction of complex NiO to Ni^0 particles interacting strongly with support (Roh *et al.*, 2002). Furthermore, the shoulder peak was attributed to the reduction of CeO_2 (Pengpanich *et al.*, 2004).

The addition of Mg does affect the reduction temperature of NiO. The reduction peaks of NiO were drastically decreased with increasing MgO loading. This might be due to that a Ni-Mg mixed oxide solid solution was formed over supported catalysts (indicated by XRD analysis) in which it is very difficult to be reduced (Yejun *et al.*, 2007). Moreover, the reduction peaks of NiO were shifted to higher temperatures with increasing MgO loading. This might be due to the strong interaction between NiO and Ni-Mg mixed oxide solid solution over CZO support requiring a higher temperature to reduce NiO to active Ni^0.

At a given loading of MgO, the catalysts prepared by sequential incipient wetness impregnation had lower NiO reducing temperature and higher amount of NiO reduction than those prepared by co-impregnation. This indicates that the catalysts prepared by sequential incipient wetness impregnation have weaker interaction between NiO and Ni-Mg mixed oxide solid solution over CZO support than those catalysts prepared by co-impregnation.

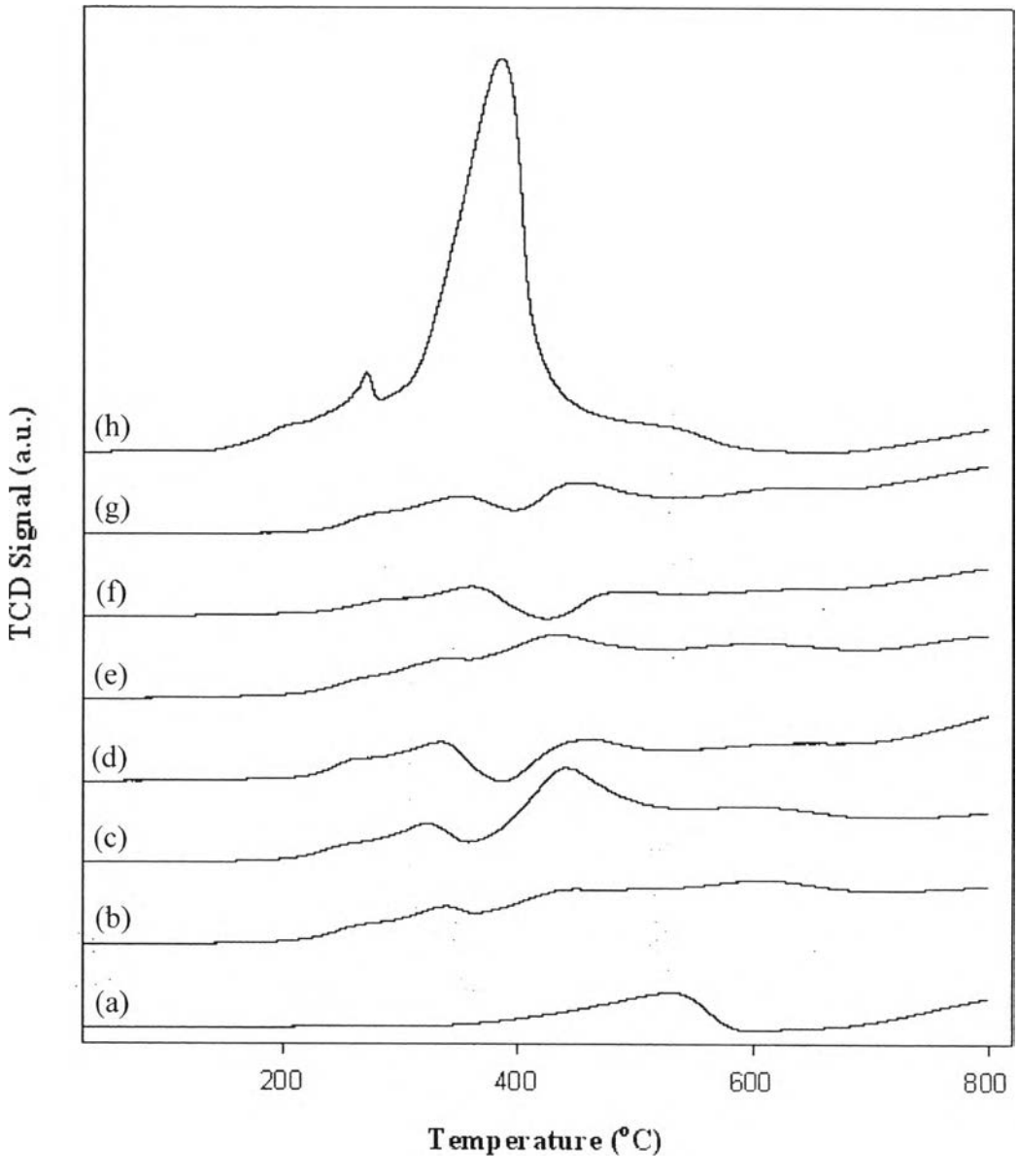

Figure 4.1 H_2-TPR profiles for the catalysts with a heating rate of 10 °C min^{-1}, a reducing gas containing 5% hydrogen in argon with a flow rate of 50 ml min^{-1}: (a) CZO, (b) 15Ni5Mg/CZO (C), (c) 15Ni5Mg/CZO (S), (d) 15Ni10Mg/CZO (C), (e) 15Ni10Mg/CZO (S), (f) 15Ni15Mg/CZO (C), (g) 15Ni15Mg/CZO (S), and (h) 15Ni/CZO (Imp.).

4.1.3 X-ray Diffraction (XRD)

XRD patterns for the NiO-MgO over CZO catalysts are shown in Figure 4.2. All the catalysts exhibit major peaks at ca. 28.8°, 33.5°, 47.5°, and 56.8° (2θ) indicating a cubic fluorite structure of CeO_2 (Pengpanich *et al.*, 2002). Small peaks of NiO were observed at ca. 37.2°, 43.3°, and 63.0° (2θ). No distinguishable peaks of MgO could be observed for the catalysts prepared. This might be due to the similar XRD patterns for both NiO and MgO (Tang *et al.*, 1998). As compared to the diffraction peaks of 15Ni/CZO, an increase in MgO loading resulted in the slight decrease in diffraction peaks of NiO at ca. 37.2°, 43.3°, and 63.0° (2θ). However, the peak intensity of NiO at ca. 43.3°, and 63.0° (2θ) was slightly increased with increasing the content of MgO, indicating that the Ni-Mg mixed oxide solid solution was formed (Yejun *et al.*, 2007). At a given loading of MgO, no distinguishable peaks for the sequential incipient wetness impregnation and co-impregnation catalysts could be observed by XRD.

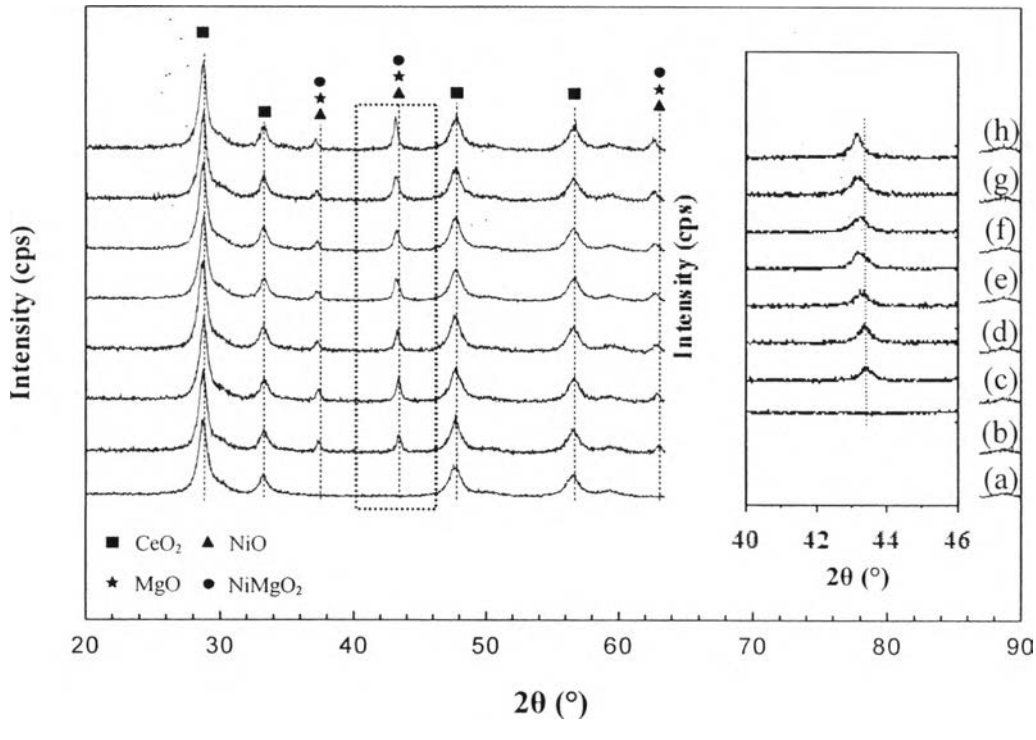

Figure 4.2 XRD patterns for the NiO-MgO over the CZO: (a) CZO, (b) 15Ni/CZO (Imp.), (c) 15Ni5Mg/CZO (S), (d) 15Ni5Mg/CZO (C), (e) 15Ni10Mg/CZO (S), (f) 15Ni10Mg/CZO (C), (g) 15Ni15Mg/CZO (S), and (h) 15Ni15Mg/CZO (C).

4.1.4 Scanning Electron Microscopy (SEM)

Figure 4.3 shows SEM images of the 15Ni/CZO, 15Ni5Mg/CZO (S), and 15Ni5Mg/CZO (C) catalysts. The NiO particle size of the samples is in the range of 20-50 nm which is similar to the average NiO particle size determined from XRD by Scherrer's equation (Table 4.2).

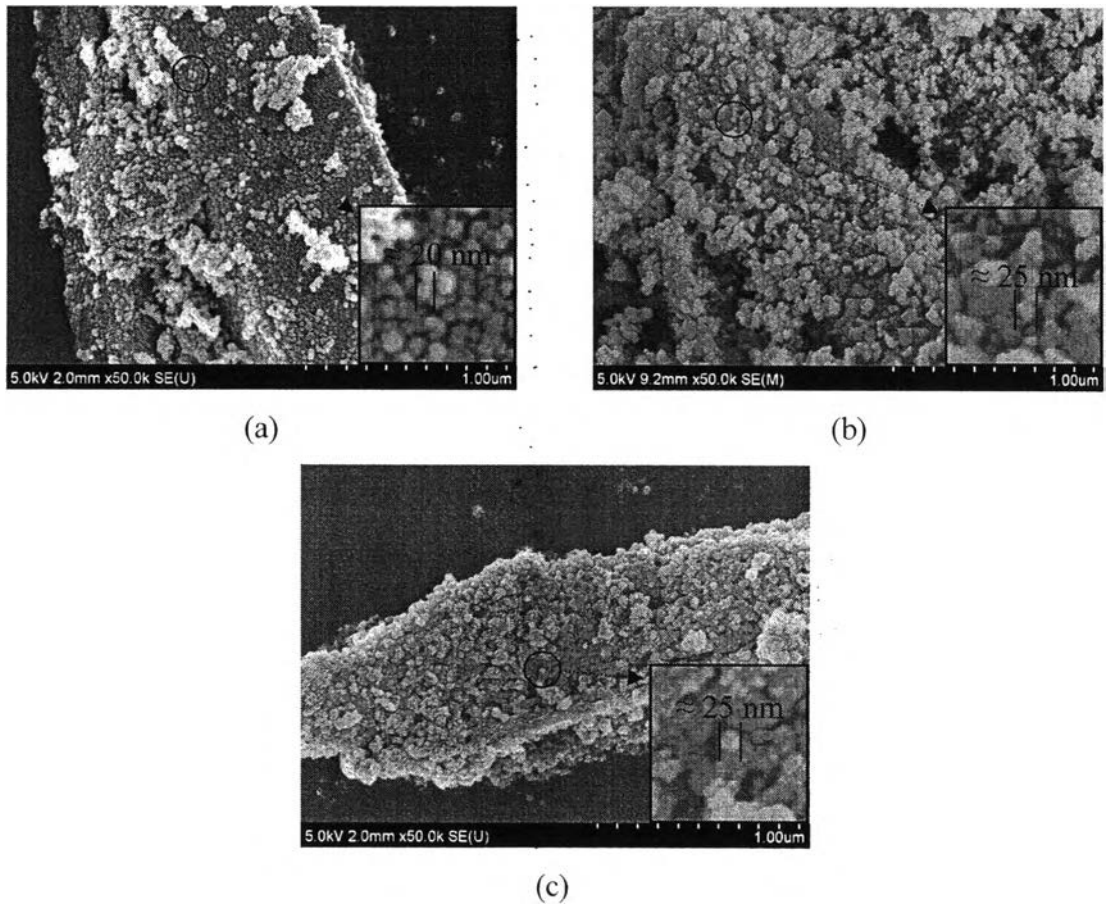

Figure 4.3 SEM images (50000x magnification) of (a) 15Ni/CZO, (b) 15Ni5Mg/CZO (S), and (c) 15Ni5Mg/CZO (C) catalysts.

Table 4.2 The average NiO particle sizes of catalysts determined from XRD by Scherrer's equation

Catalyst	Average NiO particle size (nm)
15Ni/CZO	21.16
15Ni5Mg/CZO (S)	23.33
15Ni5Mg/CZO (C)	23.31
15Ni10Mg/CZO (S)	24.42
15Ni10Mg/CZO (C)	25.22
15Ni15Mg/CZO (S)	25.75
15Ni15Mg/CZO (C)	29.18

4.2 Catalytic Activities for Methane Partial Oxidation

4.2.1 Catalytic Activity Tests

Figure 4.4 shows the light-off temperatures for MPO over the catalysts investigated. For the 15Ni/CZO catalyst, MPO is initially started at a temperature of 550 °C. Adding Mg can cause the light-off temperatures shifted to higher temperatures. For the MgO loading catalysts, MPO is initially started at a temperature of 600 °C as for 5 wt% MgO and shifted to higher temperatures with increasing MgO loading. This is because the Ni surface was partially covered with MgO, and the strong interaction between NiO and Ni-Mg mixed oxide solid solution can lead to the difficulty in reducing NiO resulting in less catalytic activity at low temperatures. The results obtained are in agreement with the degrees of metal dispersion (Table 4.1). In spite of CH_4 conversion, H_2 and CO selectivities were slightly decreased with increasing MgO loading as shown in Figures 4.5 and 4.6, respectively. However, as seen in Figure 4.6, the CO selectivity is slightly increased at temperatures beyond 650 °C when adding Mg. over. This implies that the addition of Mg can stabilize the dispersion of Ni particles beneficial to prevent the carbon deposition at high temperatures.

At a given loading of MgO, the catalysts prepared by sequential incipient wetness impregnation perform somewhat better than those prepared by co-impregnation catalysts. This is because the catalysts prepared by sequential incipient wetness impregnation possess a slightly higher metal dispersion and slightly weaker interaction between NiO and Ni-Mg mixed oxide solid solution over CZO.

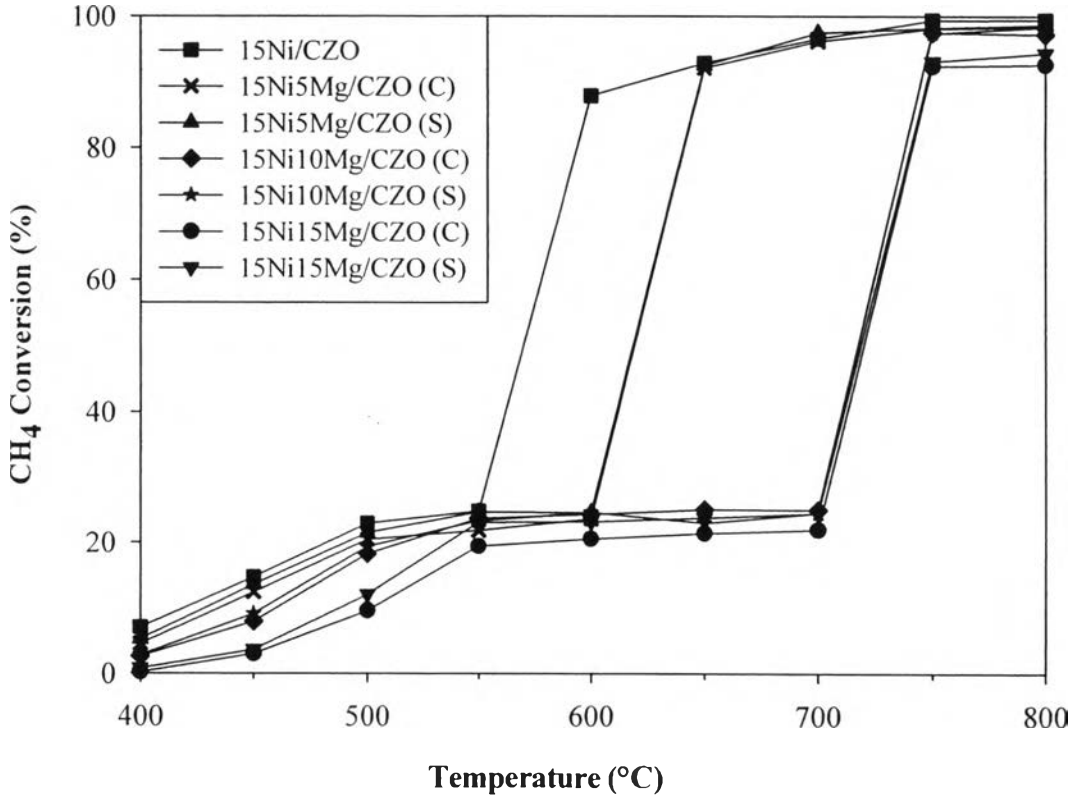

Figure 4.4 Light-off temperatures (CH_4 Conversion) over the catalysts investigated (CH_4/O_2 ratio of 2:0, GHSV = 53000 h^{-1}).

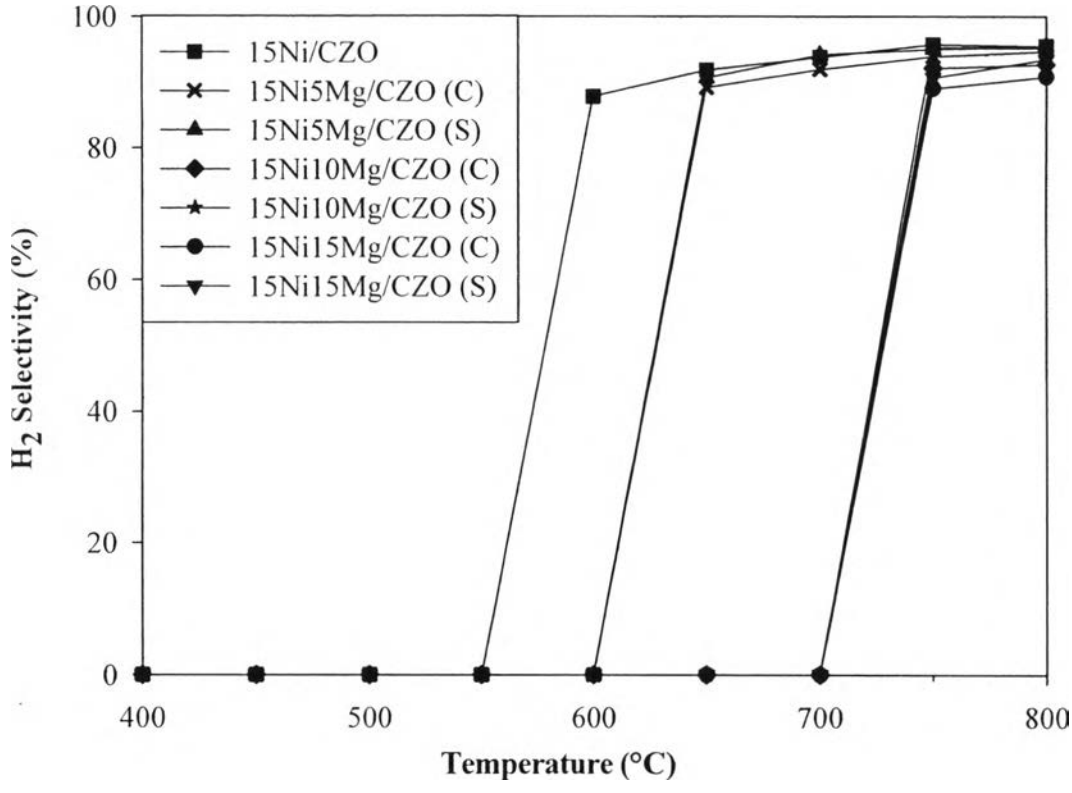

Figure 4.5 H_2 Selectivity over the catalysts investigated (CH_4/O_2 ratio of 2:0, GHSV = 53000 h^{-1}).

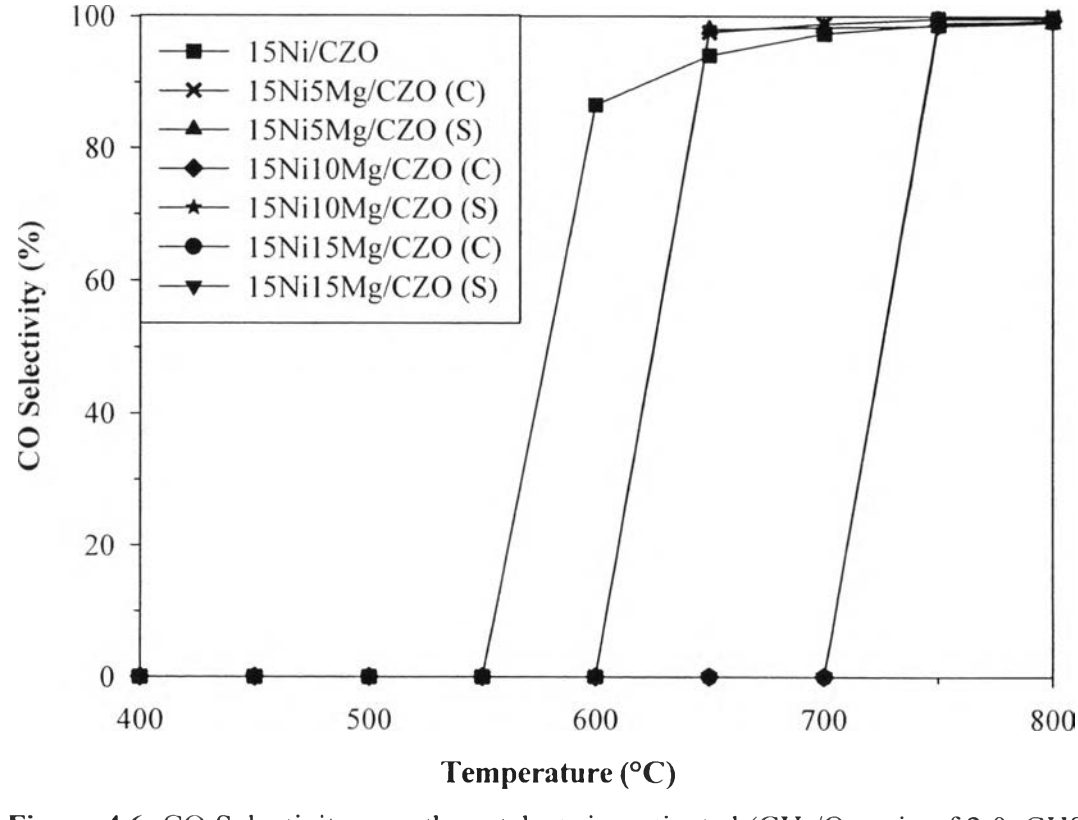

Figure 4.6 CO Selectivity over the catalysts investigated (CH_4/O_2 ratio of 2:0, GHSV = 53000 h^{-1}).

4.2.2 Carbon Deposition on Catalysts and Catalyst Stability

Due to their higher catalytic activities as compared with the others, the 15Ni5Mg/CZO (C) and 15Ni5Mg/CZO (S) catalysts were selected to further investigate on carbon deposition and their stability under specified reaction conditions.

Figure 4.7 presents the TPO profiles of the catalysts investigated after reaction at 750 °C. All the spent catalysts show peaks centered at about 370 and 720 °C. It is suggested that the first peaks at temperature about 320 °C could be described to amorphous carbon, and the second peaks at temperature about 720 °C could be described to graphitic carbon (filamentous carbon). The results are similar to that observed by Pengpanich *et al.* (2004) suggesting that the peaks observed on the TPO profiles can be due to the presence of different types of carbon or different sites of carbon deposition.

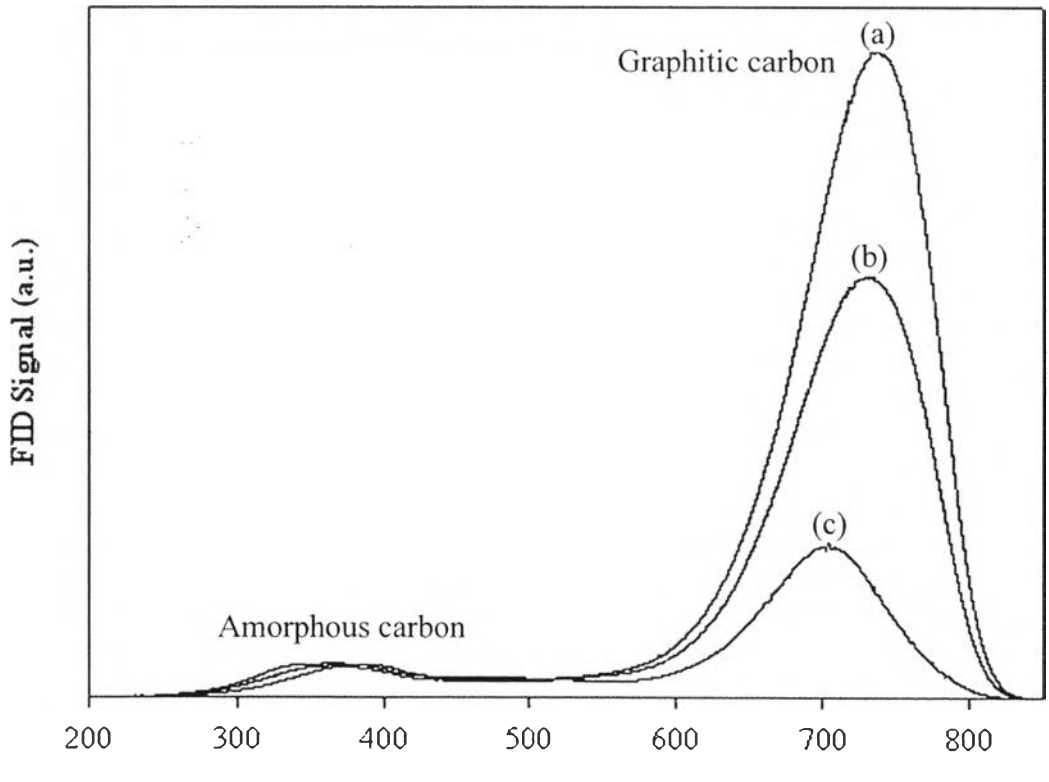

Figure 4.7 TPO profiles of catalysts after reaction at 750 °C (CH_4/O_2 of 2:0, GHSV = 53000 h^{-1}) an oxidizing gas containing 2% oxygen in He with a flow rate of 40 ml/min: (a) 15Ni/CZO, (b) 15Ni5Mg/CZO (C), and (c) 15Ni5Mg/CZO (S).

As shown in Figure 4.8, the filamentous carbon was mainly formed on the spent catalysts whereas the amorphous carbon cannot be observed from SEM images. The results are in agreement with the main type of carbon deposition which was measured by TPO technique (Figure 4.7).

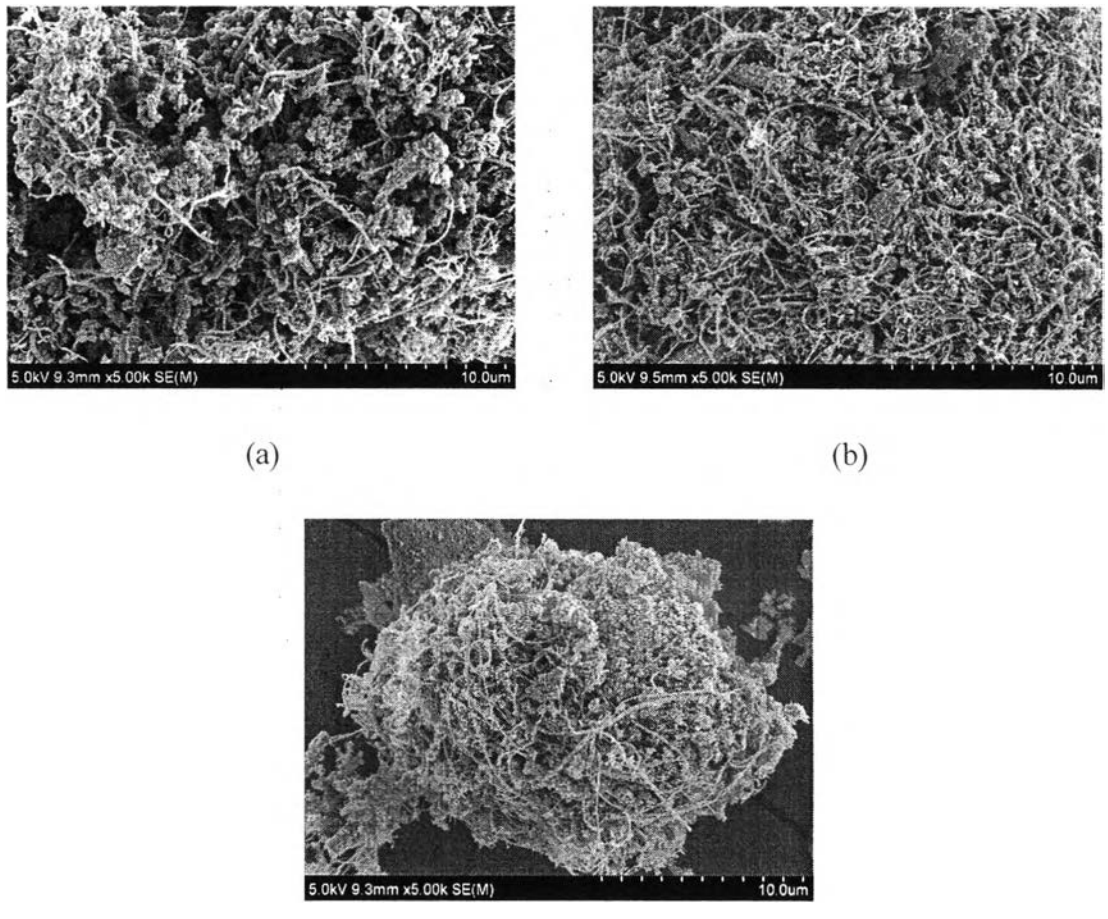

Figure 4.8 SEM images (5000x magnification) of filamentous carbon of (a) 15Ni/CZO, (b) 15Ni5Mg/CZO (C), and (c) 15Ni5Mg/CZO (S) spent catalysts after exposure to MPO reaction at 750 °C (CH_4/O_2 = 2:0, GHSV = 53000 h^{-1}) for 18 h.

Figure 4.9 presents SEM images of the spent catalysts after exposure to MPO reaction at 750 °C. In comparison with SEM images in Figure 4.3, the Ni particle size of the 15Ni/CZO spent catalyst was dramatically increased (20 – 280 nm) after a reaction time of 18 hours at 750 °C whereas the Ni particle size of the 15Ni5Mg/CZO (C) spent catalyst was slightly increased (50-100 nm) but that of the 15Ni5Mg/CZO (S) spent catalyst remained unchanged (20-40 nm). It can be concluded that the addition of Mg could prevent the agglomeration of Ni particles at high temperatures, and the 15Ni5Mg/CZO (S) seems to be most suitable catalyst composition as for preventing the carbon deposition due to its highest metal dispersion degree and smallest Ni particles at high temperatures.

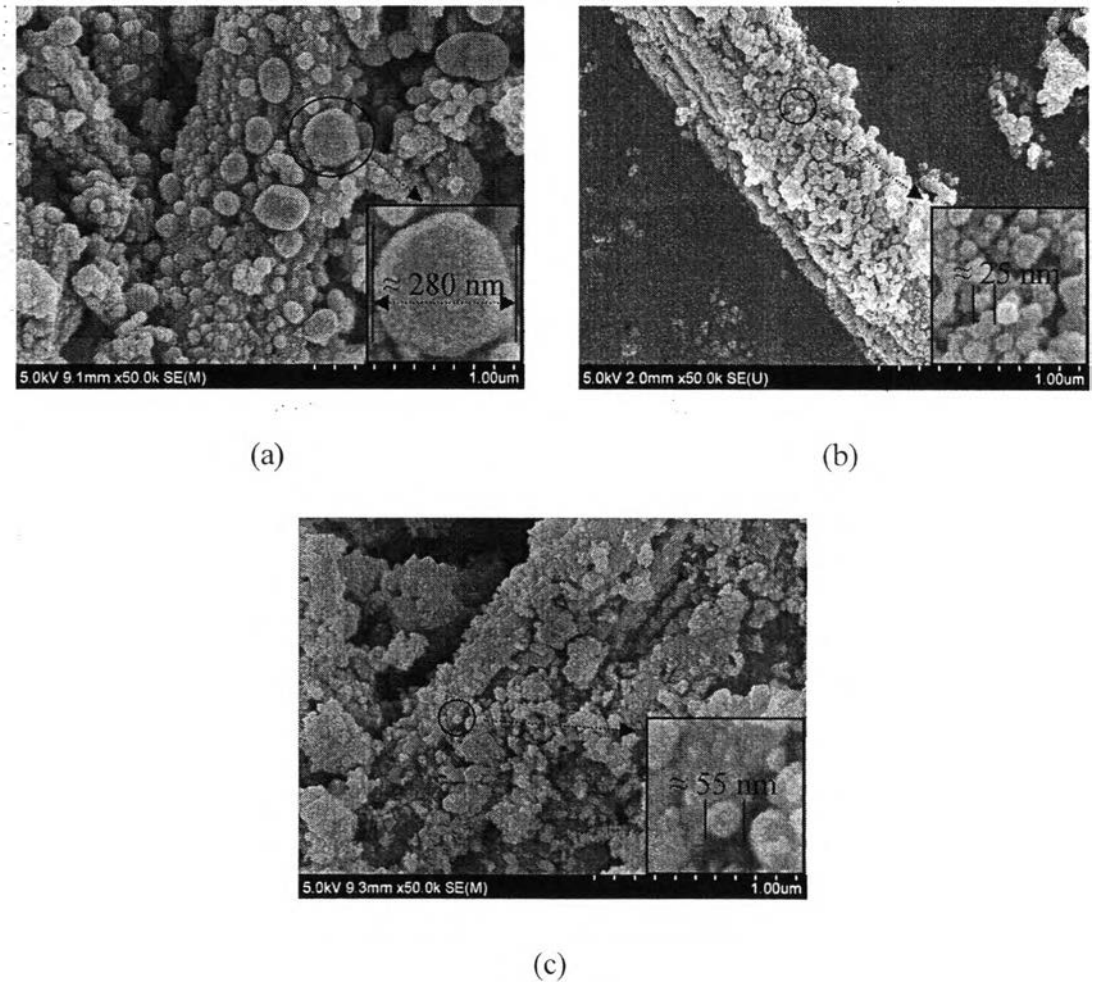

Figure 4.9 SEM images (50000x magnification) of (a) 15Ni/CZO, (b) 15Ni5Mg/CZO (S), and (c) 15Ni5Mg/CZO (C) spent catalysts after exposure to MPO reaction at 750 °C (CH_4/O_2 = 2:0, GHSV = 53000 h^{-1}) for 18 h.

Table 4.3 Carbon deposition amount measured by TPO over the catalysts after 18 hours of reaction at 750 °C and a CH_4/O_2 ratio of 2

Catalyst	Amount of carbon deposition (wt%)
15Ni/CZO	32.17
15Ni5Mg/CZO (C)	22.23
15Ni5Mg/CZO (S)	9.54

The amounts of carbon deposition on the catalysts after a reaction time of 18 hours at 750 °C and a CH_4/O_2 ratio of 2 determined by TPO technique are shown in Table 4.3. The amount of carbon deposition on the 15Ni/CZO spent catalyst was 32.17 wt% whereas those of carbon deposition on the 15Ni5Mg/CZO (C) and 15Ni5Mg/CZO (S) spent catalysts were 22.23 and 9.54 wt%, respectively. It is indicated that the strong interaction between Ni particles and Ni-Mg mixed oxide solid solution could prevent the agglomeration of Ni particles at high temperatures, which helped suppress the carbon deposition on the catalysts. This is because the carbon deposition is easy to deposit on a larger ensemble of active Ni sites (Trimm *et al.*, 1999). This is confirmed by SEM images (Figure 4.9) and metal dispersion degrees of the catalysts (Table 4.1).

At the same operating conditions, carbon formation on the 15Ni5Mg/CZO (S) was significantly less than that of the 15Ni5Mg/CZO (C). This can be attributed to a higher metal dispersion for the 15Ni5Mg/CZO (S) at a higher temperature.

Figures 4.10 - 4.12 illustrate the methane conversion, hydrogen selectivity, and carbon monoxide as well as carbon dioxide selectivity for the catalysts investigated, respectively. Accordingly, CH_4 conversion and H_2 selectivity for the 15Ni/CZO and 15Ni5Mg/CZO (C) catalysts remain unchanged whereas their CO selectivity is slightly decreased but CO_2 selectivity is slightly increased with increasing time on stream for MPO reaction at 750 °C. This is because the Boudouard reaction ($2CO \rightarrow C+CO_2$) might occur during the course of reaction. Moreover, a plugging of the reactor was observed for the 15Ni/CZO catalyst after 18 hours on stream resulting from the rapid and heavy coke formation. The results are in agreement with the amount of carbon deposition which was measured by TPO technique as shown in Table 4.3. However, the catalytic activity for the 15Ni5Mg/CZO (S) catalyst remains unchanged with increasing time on stream for MPO reaction at 750 °C. It is apparent that the 15Ni5Mg/CZO (S) could diminish the Boudouard reaction resulting in the stability of the catalyst.

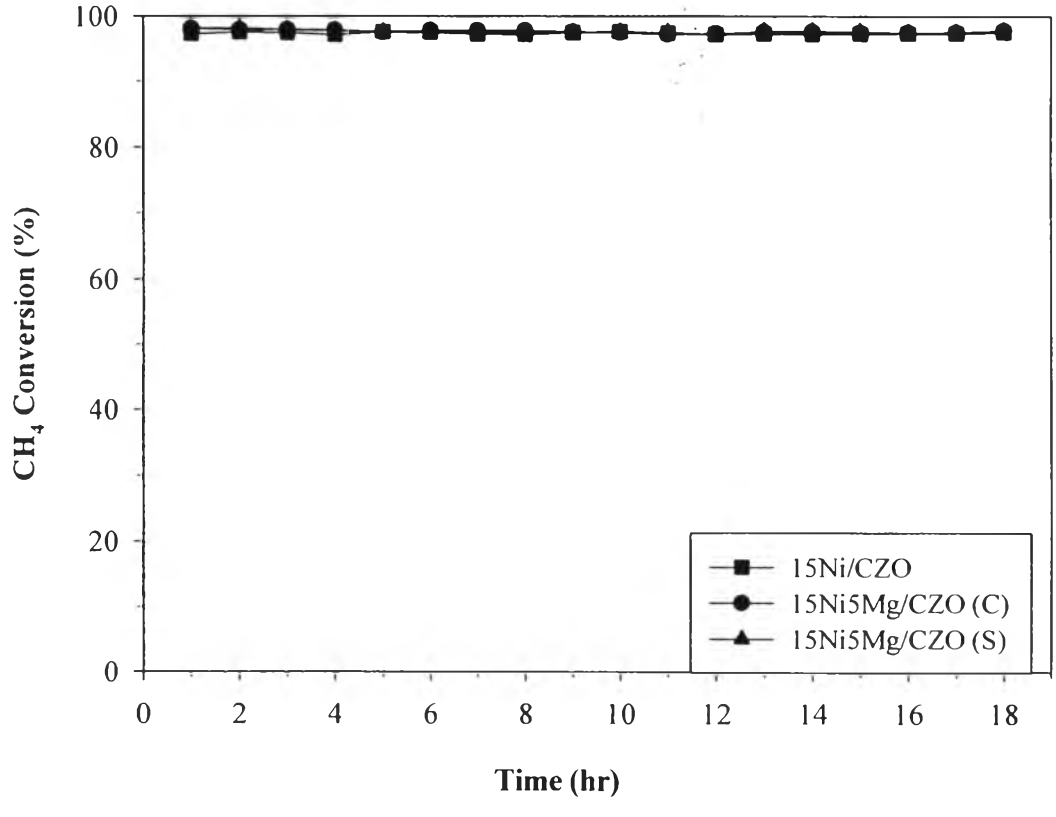

Figure 4.10 CH_4 conversion as a function of time over the catalysts investigated at 750 °C (CH_4/O_2 ratio of 2:0, GHSV = 53000 h^{-1}).

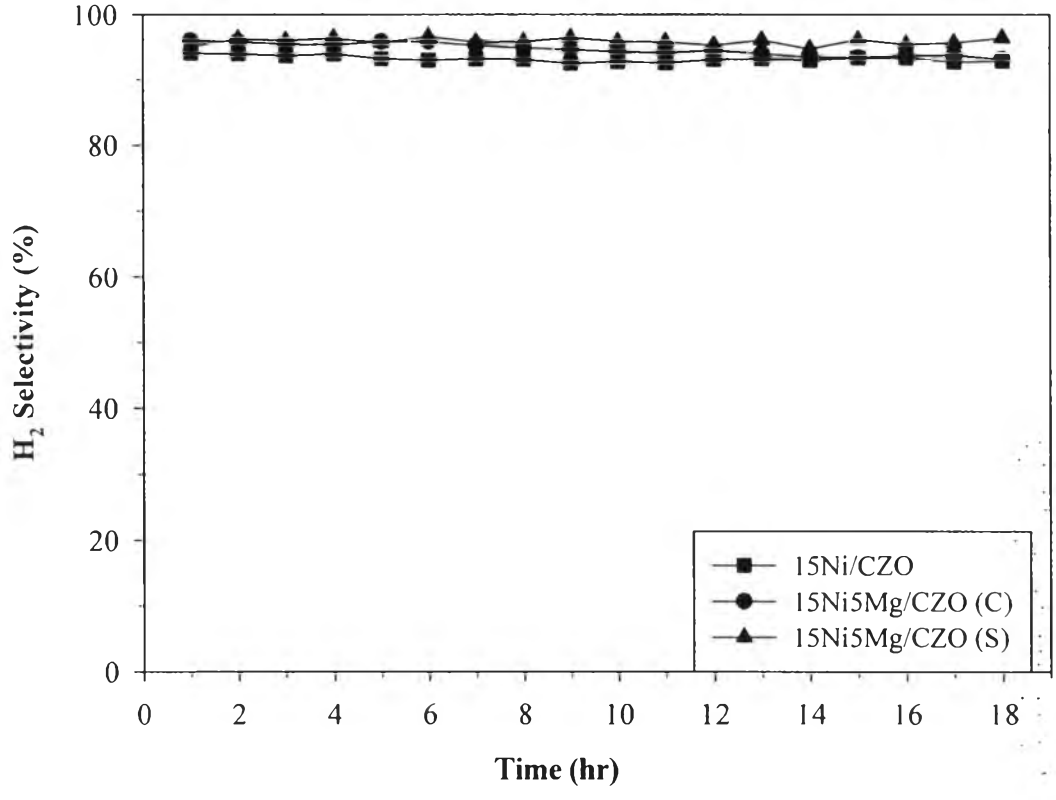

Figure 4.11 H_2 Selectivity as a function of time over the catalysts investigated at 750 °C (CH_4/O_2 ratio of 2:0, GHSV = 53000 h^{-1}).

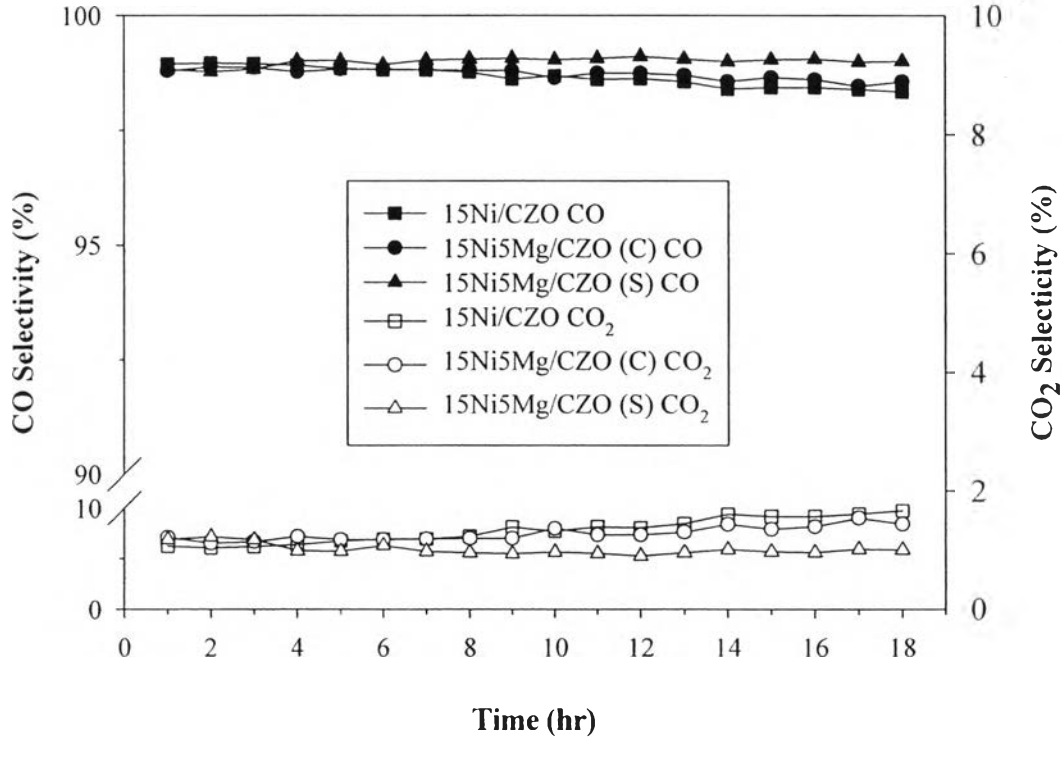

Figure 4.12 CO and CO_2 selectivities as a function of time over the catalysts investigated at 750 °C (CH_4/O_2 ratio of 2:0, GHSV = 53000 h^{-1}).

Figure 4.13 shows the H_2/CO ratios as a function of time for the catalysts studied. An appropriate H_2/CO ratio of 2 is consistently obtained for the 15Ni5Mg/CZO (S) catalyst whereas H_2/CO ratios for the 15Ni/CZO and 15Ni5Mg/CZO (C) catalysts are slightly increased with increasing time on stream due to the decreased CO selectivity.

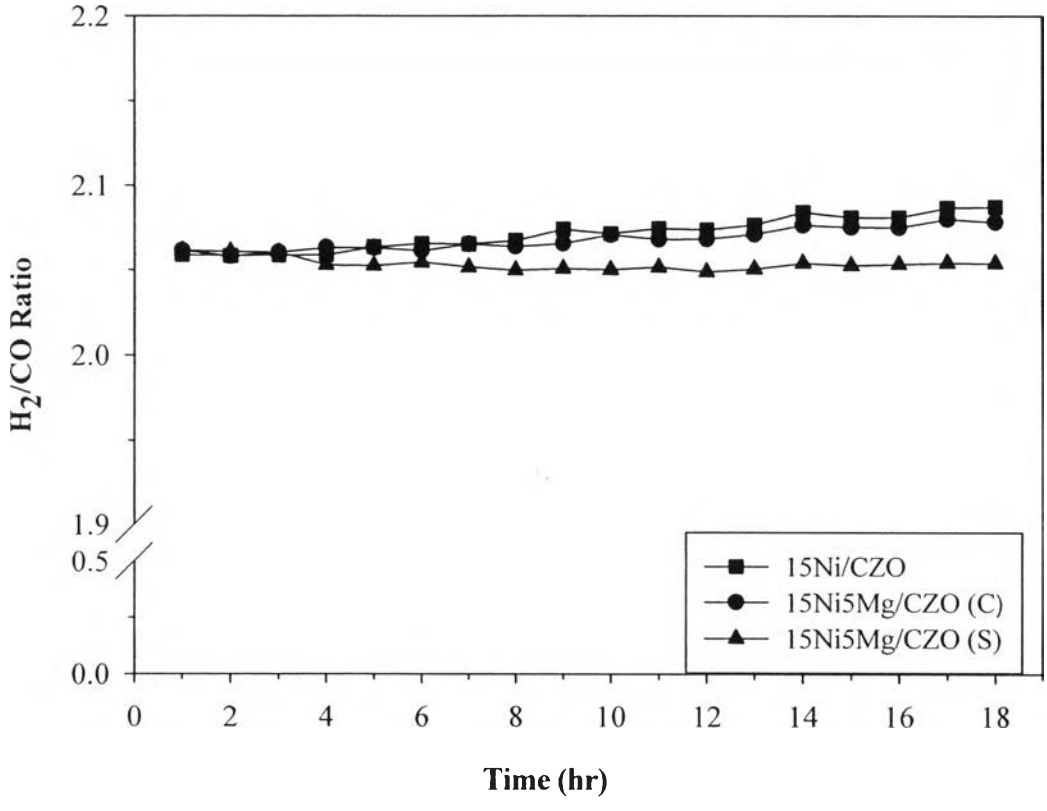

Figure 4.13 H_2/CO ratio as a function of time over the catalysts investigated at 750 °C (CH_4/O_2 ratio of 2:0, GHSV = 53000 h^{-1}).